Investigation of Loop Seal Pressure in Circulating Fluidized Bed: A Comparative Analysis of Biomass Combustion

Hidayat, Taopik
Research Center for Energy Conversion and Conservation, National Research and Innovation Agency

Budianto, Dwika
Research Center for Energy Conversion and Conservation, National Research and Innovation Agency

Kurniawati, Desy
Research Center for Energy Conversion and Conservation, National Research and Innovation Agency

Ahda, Yusuf
Research Center for Energy Conversion and Conservation, National Research and Innovation Agency

他

https://doi.org/10.5109/7236914

出版情報：Evergreen. 11 (3), pp.2755-2760, 2024-09. Interdisciplinary Graduate School of Engineering Sciences, Kyushu University, Japan
バージョン：

Investigation of Loop Seal Pressure in Circulating Fluidized Bed: A Comparative Analysis of Biomass Combustion

Taopik Hidayat[1,*], Dwika Budianto[1], Desy Kurniawati[1], Yusuf Ahda[1], Ilham Arnif[3], Anita Dewi Limbong[1], Nur Endah Eny S.[1], Wiwie Chaeruni[1,2], Riko Ardiana[3], Cahyadi[1]

[1]Research Center for Energy Conversion and Conservation, National Research and Innovation Agency, Tangerang Selatan, Indonesia

[2]Master Programs of Energy, School of Postgraduate Studies, Diponegoro University, Semarang, Indonesia

[3]Energy Conversion Laboratory, National Research and Innovation Agency, Tangerang Selatan, Indonesia

*Author to whom correspondence should be addressed:
E-mail: taop001@brin.go.id

(Received May 13, 2024: Revised August 12, 2024: Accepted August 19, 2024).

Abstract: The purpose of this research is to investigate the effect of adding ash to the loop seal in a 15 kW_{th} CFB. This experimental test comprised three distinct trials, each utilizing 2,500 grams of sand and the incorporation of 50 and 100 grams of biomass ash, respectively. The experimental results show that the addition of ash to the loop seal affected the operational performance. the circulation rate did not occur due to voids in the loop seal when 100 grams of ash was added. This research provided insight into the effects of full biomass firing in CFB boilers.

Keywords: circulating fluidized bed; circulation rate; loop seal; solid particle

1. Introduction

Global warming and environmental emissions issues are the main challenges for developing power plants in these countries. One effort to overcome these environmental problems is implementing Net Zero Emission (NZE).

According to Notosiswoyo Sudarto, 2011, In Indonesia, coal remains the primary and most significant energy source[1)]. Burning fossil energy can potentially increase pollutants, contributing to global warming[2-4)]. Moreover, in Handbook of Energy & Economic Statistics of Indonesia, mentioned that over 50% of Indonesia's total installed generating capacity, or around 46 GW, are steam power plants[5)]. Therefore, Indonesia needs to develop a strategy to realize NZE by 2060[6,7)]. Indonesia will transition to clean energy by establishing several new renewable energy policies. Gradually, existing coal-fired power plants will be retired[8)]. Cofiring biomass has been investigated to minimize fossil fuel consumption due to reducing the emission and the scarcity of fossil fuel[9-11)]. Cofiring biomass using a Circulated Fluidized Bed has been studied although several treatments should be required[12-14)]. Existing coal-fired power plants with circulating fluidized beds will face some challenging issues in terms of both operational procedures and maintenance requirements when converting a coal combustion power plant to full biomass fuel[15, 16)].

The performance of CFB boilers, the combustion fractions, and temperature distributions will all be directly impacted by the quality of solid circulation rate, gas velocity, and bed pressure drop in the loop seal[17-19)]. The loop seal, a particle recycling mechanism used in CFB reactors, is one of the most critical parts of the CFB[20-22)]. The loop seal is one of the nonmechanical valves that can control solid flow by aeration[23-25)]. In the CFB, when the loop seal fails, solids accumulate in the standpipe and cyclone, blocking the recirculation of the solids around the CFB loop, which shuts down the boiler[20, 26, 27)].

Most researchers use the sand and glass bead as solid particles in the loop seal for the cold model simulation. However, when CFB is operating (hot model simulation) there must be ash circulated together with the sand in the loop seal[28)]. Therefore, more comprehensive research is needed to investigate the phenomena of added ash and sand in the seal loop[28, 29)]. This study is focusing on biomass ash. Many studies vary the size of the loop seal but in this study, the dimensions of the loop seal are made constant to see how significant the effect of added ash in the loop seal. The experiment setup uses 3 stages sequentially. In stage 1, the loop seal was conditioned with 100% sand (S), and the circulation rate was kept stable by adjusting the fluidizing air in the supply chambers (SC) and recycle chambers (RC). Stage 2 was carried out by adding 50 grams of ash (about 2% of total sand mass) into the stage 1 (S50A). A further 50 grams were then added to the stage 2 for stage 3 (S100A). Each stage was running for 1 hour to ensure the circulation in the CFB was stable. The current study aimed to discover the effect of adding biomass ash into the loop seal to estimate the impact of bed material on switching from coal to biomass fuel in power plants.

Research related to this cold model mostly uses glass bed or sand bed material. The material circulates homogeneously. However, in previous studies, ash has not been considered as a side product of hot model combustion. The focus of this research is to determine the effect of ash with a mixture of sand bed and 100% sand bed on combustion circulation in the hot model. It is expected that this condition is close to the ideal condition in the process.

Table 1. Study literature of circulating fluidized bed

Author	Years	Particle Size (μm)	Density (kg/m³)	Velocity (m/s)	Model Configuration (m)
Bolland et al(30)	2001	117	3,320	5.6-7.2	0.411x8.5
Fan et al(31)	2008	62	1,747	2.2-3.7	0.009x5
Li et al(32)	2011	60	1,370	1.0-2.0	0.076x10.2
Li et al(33)	2013	60	1,370	1.0-2.0	0.076x10.2
Current work	2024	177 - 297	1,288	3.2-6.6	0.076 x 3

2. Material and Method

2.1. Material

The materials used in this research were silica sand and biomass ash. In the initial condition (stage 1), the sand material was conditioned in two locations (main grate and loop seal). The sand was shieved using two mesh sizes which are 50-mesh (297 μm) and 80-mesh (177 μm). These sizes were following the CFB particle size range of 50 - 500 μm (31). The ash was sieved using 50-mesh and 80-mesh as same as the sand treatment but the ash less than 80-mesh was included.

2.2 Method

The cold model simulator used acrylic with a diameter of the main grate of 3 in (75 mm) and a height of 3,000 mm from the grate as shown in Fig.1. Main grate is a perforated plate type with fine wire mesh sandwiched with 2 perforated plates.

Table 2. Bulk density and mass of particles according to sieve sizes

Particle size	Bulk density	Mass
[-]	[kg/m³]	[gram]
Main grate		
177 - 297 μm	1,252	500
> 297 μm	1,300	1,500
Total	1,288 (avg)	2,000
Initial loop seal/sand only (stage 1) – S		
177 - 297 μm	1,252	125
> 297 μm	1,300	375
Total	1,288 (avg)	500
Ash added into main bed (stage 2) – S50A		
< 177 μm	253	17.5
177 - 297 μm	180	12.5
> 297 μm	140	20
Total	189 (avg)	50
Ash added into main bed (stage 3) – S100A		
< 177 μm	253	17.5
177 - 297 μm	180	12.5
> 297 μm	140	20
Total	189 (avg)	50

The wire mesh protects against leakage when shut down, so the solid particles will stay above the grate. The cold model simulator was designed for use in a 15 kW_{th} CFB. The pressure transducer with a measurement range of 0 – 10 kPa was installed into the air box under the main grate (P_m) to simulate the pressure in the CFB boiler air box of the main grate. The pressure transducer with the same range is also mounted in the two air boxes below SC and RC as same as the SC and RC of CFB boilers. All of these three transducers measured the static pressure for each location. To determine velocity during bubbling and fast bed conditions, the differential pressure transducer with a measurement range of 0 – 1 kPa was mounted in the riser at a height of 1,500 mm from the main grate. The differential pressure (Pr) measurement results are converted to velocity using the following equation

$$v = \sqrt{2\Delta P} \qquad (1)$$

where v is velocity (m/s) and ΔP is differential pressure (Pa). All pressure transducers were connected to a data logger and recorded during the test for stage 1, stage 2, and stage 3.

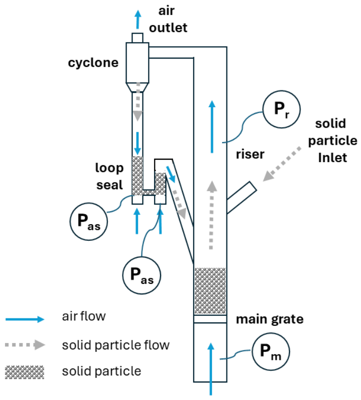

Fig. 1 CFB schematic diagram

The study began with no fluidizing air introduced, followed by the introduction of fluidizing air to the main grate, which produced a static pressure of 4 to 6 kPa (P_m)[37]. The sand in the main grate starts in a static position, then moves to bubbling and finally to fast bed or circulating as the fluidizing air to the main grate increases. The loop seal had fluidizing air for each SC and RC. The SC is the chamber that contains the solid particles returned from the cyclone, while the RC contains the recycle chamber that flows from the supply chamber to be returned to the main grate through a fluidization process. The fluidizing air to the SC and RC starts when the sand from the main grate has reached the circulating state, characterized by the sand starting to fall from the cyclone to the SC. The fluidizing air to the SC and RC is adjusted to maintain the sand level in the SC between a height of 22 cm as LL and 25 cm as UL, ensuring a balanced flow of solid particles entering the SC and exiting the RC. The loop seal dimensions according to Fig. 2 are presented in Table 3.

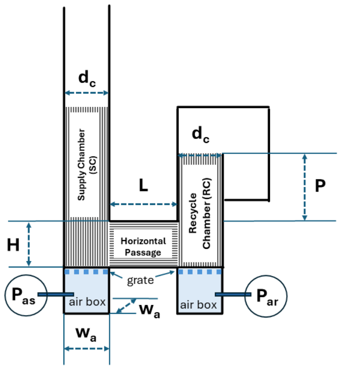

Fig. 2 Loop seal nomenclature

Table 3. Loop seals dimension

Parameter	Dimension (mm)
H	20
L	50
P	215
w_a	34
d_c	37

3. Result and discussion

Solid particles could be classified according to the Geldart diagram depending on particle diameter and particle density[38, 39]. In this case, ash was classified as group C or the cohesive type, which was challenging to fluidize and had the potential for channeling in the bed. On the contrary, sand was classified as group A which had better fluidization characteristics[40, 41].

Table 4. Study literature of particle properties

Author	Years	Geldart Group	Material	Density (kg/m³)	dp (µm)
Chew et al[34]	2011	B	Polystyrene (PS)	1,050	327.5
		B	Glass Bead	2,500	165
		B	Sand	2,650	196
Xu and Zhu[35]	2011	B	Glass Bead (i)	2,403	134
		B	Glass Bead (ii)	2,498	288
		B	Sand (iii)	2,467	138
Kiani et al[36]	2013	B	Glass Bead (ii)	2,500	170
		B	Glass Bead (iii)	2,500	650
		B	Glass bead (i)	2,640	150
		B	Glass bead (ii)	2,640	300
Current work	2024	B	sand	1,252	177-297
		B	sand	1,300	>297
		C	ash	189	164
		B	sand and ash (2% of total sand)	253	<177
		B		180	177 - 297
		B		140	>297
		B	sand and ash (4% of total sand)	253	<177
		B		180	177 - 297
		B		140	>297

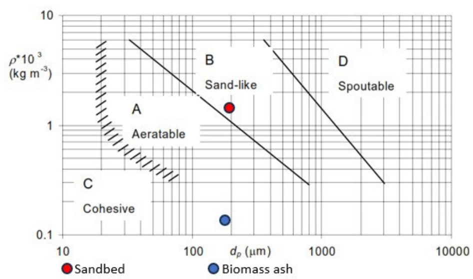

Fig. 3 The distribution plot of sand bed particles and biomass ash, in the Geldart diagrams[38]

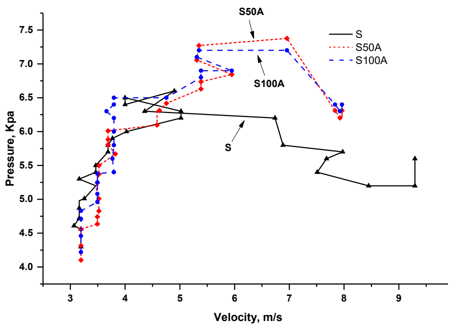

Fig. 4 The correlation between velocity and main grate pressure

Table 4. describes the particle properties and materials used in CFB research conducted by previous researchers against the focus of the current research. Based on the Geldart diagrams, most of the materials in this research are in the B material classification.

The correlation between velocity and static pressure in the main grate for each stage can be seen in Fig. 4. During the start bubbling condition, P_m was higher at stage 2 and stage 3 compared to stage 1, at 4.93 kPa and 5.38 kPa, respectively as shown in Table 5. The minimum velocity also increased to 3.5 m/s. The increased pressure in the main grate indicates a greater need for pressure from the fluidizing air source to fluidize the solid particle. During the start circulating condition, P_m is lower at stage 2 and stage 3 compared to stage 1, at 5.4 kPa and 6 kPa, respectively. Similarly, the minimum velocity decreases to 3.5 m/s and 3.8 m/s. It can be seen that the addition of ash can affect the minimum velocity in bubbling and circulating conditions on the main grate. The greater the amount of ash added to the sand, the higher the minimum velocity required for the solid particle to enter the bubbling condition.

Table 5. Pm and velocity for start bubbling and circulating condition for each stage.

Stage	Start Bubbling		Start Circulating	
	P_m (kPa)	v (m/s)	P_m (kPa)	v (m/s)
1	4.61	3.2	6.6	6.6
2	4.93	3.5	5.4	3.5
3	5.38	3.5	6	3.8

At stage 2 and stage 3, since the solid particles already contain ash, which has a lower density than sand and enters the SC, there is a decrease in P_m. P_m decreases when the velocity rises to 4.8 m/s in stage 3. The solid particles from the loop seal do not return to the main grate due to the disruption of solid circulation in the loop seal. The particles are difficult to move from SC to RC. As a result, the particles accumulate in the SC chamber and create a void between the SC and RC grates. Finally, the quantity of solid particles on a main grate has decreased. Channeling also occurs in the solid particles before reaching the bubbling condition in stage 2 and stage 3. This result confirms the findings of Yandaizhi[23)], who reported that the Geldart C particle group is hard to fluidize and prone to channeling.

As shown in Fig. 5, in stage 1, static pressure in SC air box (P_{as}) and static pressure in RC air box (P_{ar}) are relatively stable at all velocities, averaging 3 kPa and 2.4 kPa, respectively. P_{as} in stage 2 is lower than in stage 1 due to the lower density of particles from ash that enter the SC. Less pressure is required to lift the solid particles than the stage 1. P_{as} increasing from 1.7 kPa to 2.2 kPa as the increasing of velocity, so the air required in the supply chamber increases[42)]. In RC, fluidizing air required to fluidize the particles is higher than in stage 1 to maintain solid particle height between UL and LL, resulting in P_{ar} as the velocity increases, starting at 1.5 kPa and ending at 3.5 kPa. It indicates that the circulating flow rate is higher than in stage 1 due to smaller-sized and lower-density particles from ash that can easily be carried by air and circulated to the loop seal. This result is consistent with Leming's study[43)], which states that as the particle size decreases, the flow rate of solid particles in the loop seal will increase.

At stage 3, P_{as} is lower than in stage 2, starting at 1.3 kPa. This is due to more ash being added than stage 2 which had lower density entering the SC. However, as the velocity increases, starting at a velocity of 3.8 m/s, P_{as} decreases within a range of 0.8-1 kPa, solid particle stack up in SC exceeds UL and void is created above SC grate. The void height at the end of the test is the same as H and the length is the same as L. Lower density, smaller particle size and pressure from the main grate through the loop seal make it difficult for particles to descend to the SC grate.

P_{ar} starts at 1.3 kPa, the same as P_{as}. P_{ar} stabilizes at 1.5 kPa when velocity increases from 5.4 m/s. This is because solid particles flows from SC to RC is disrupted, so the amount of solid particles fluidized in RC decreases. At the end of the test, RC is empty. The phenomena for each stage are illustrated in Fig. 6.

In addition, after stage 3 is complete, a re-screening of solid particles was performed to determine any changes in particle distribution, as presented in Table 6. It can be observed that the number of particles smaller than 177 µm increased after the cold model test.

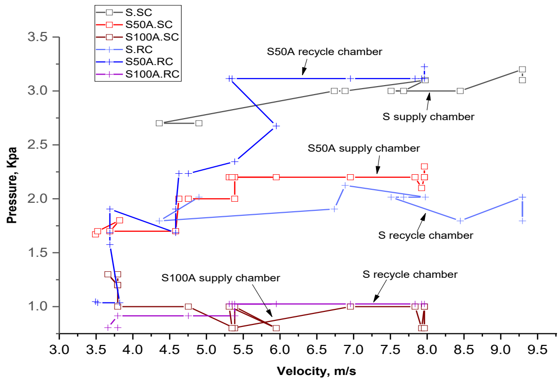

Fig. 5 P_{as} and P_{ar} in loop seal according to velocity

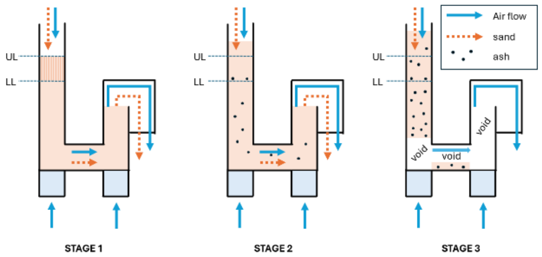

Fig. 6 Loop seal phenomena for each stage

Table 6. The solid particle distribution in the main grate after stage 3

Size	Before test (grams)	After test (grams)
< 177 µm	35	432
177 – 297 µm	525	143
> 297 µm	1,540	1,525

4. Conclusion

The addition of biomass ash can affect the performance and operation of the loop seal. Adding 50 grams of ash can initiate the circulating condition earlier, causing the SC and RC pressure operation to start earlier than using sand alone. The required pressure to lift particles is reduced in the supply chamber. However, the required pressure to fluidize particles is increased in the recycle chamber due to the high circulating rate in the loop seal. When 100 grams of ash are added, the process of circulating particles is disrupted, as indicated by the difficulty of solid particles falling into the SC grate, resulting in particles not flowing into the recycle chamber and creating a void. It is essential to limit the amount of ash that circulates in the CFB boiler to prevent disruption of the particle circulation process. This research is helpful for power generation industries, especially those using CFB boilers. It provides insight into the effects of full firing with biomass.

Acknowledgments

This work was supported under the framework of the Research Center for Energy Conversion and Conservation, National Research & Innovation Agency (BRIN) Indonesia.

Nomenclature

P_m	Static pressure in the main grate air box
SC	Supply chamber
RC	Recycle chamber
P_r	Differential pressure in the riser
V	Velocity
ΔP	Differential pressure
LL	The lower limit of solid particle height
UL	The Upper limit of solid particle height
H	Horizontal passage height in loop seal
L	Horizontal passage length in loop seal
P	Recycle chamber height
w_a	Loop seal air box width
d_c	Chamber diameter
P_{as}	Static pressure in the supply chamber air box
P_{ar}	Static pressure in the recycle chamber air box
dp	Diameter particle size

References

1) Notosiswoyo S, Iskandar I. Contribution of coal mine and coal fired power plant to CO2-emission in Indonesia. 2011.
2) Vatalis KI, Charalampides G, Platias SJPE, Finance. CCS Ready innovative technologies in coal-fired power plants as an effective tool for a Greek low carbon energy policy. 2014;14:634-43.
3) Wang L, Karimi N, Sutardi T, Paul MCJATE. Numerical modelling of unsteady transport and entropy generation in oxy-combustion of single coal particles with varying flow velocities and oxygen concentrations. 2018;144:147-64.
4) Lestari NmA. Reduction of co_2 emission by integrated biomass gasification-solid oxide fuel cell combined with heat recovery and in-situ co_2 utilization. 2019.
5) Indonesia MoeamRRo. Handbook Of Energy & Economic Statistics of Indonesia 2021. Jakarta2019.
6) Wahid A, Mustafida R, Husnil A. Exergy analysis of coal-fired power plants in ultra supercritical technology versus integrated gasification combined cycle. 2020.
7) Umar HA, Sulaiman SA, Majid MAB, Said MA, Gungor A, Ahmad RK. An outlook on tar abatement, carbon capture and its utilization for a clean gasification process. 2021.
8) Sutardi T, Wang L, Karimi N, Paul MC. Utilization of H_2O and CO_2 in Coal Particle Gasification with an Impact of Temperature and Particle Size. 2020.
9) Muhammad R, Adityosulindro S. Biosorption of brilliant green dye from synthetic wastewater by modified wild algae biomass. 2022.
10) Naryanto RF, Enomoto H, Delimayanti MK, Musyono ADNI, Naryaningsih A. Tar characteristics as influenced by air flow rate changes in a downdraft gasifier. 2023.
11) Wander PR, Bianchi FM, Caetano NR, Klunk MA, Indrusiak MLSJE. Cofiring low-rank coal and biomass in a bubbling fluidized bed with varying excess air ratio and fluidization velocity. 2020;203:117882.
12) Bernhardt D, Beckmann MJF. Simplified process model for CFB combustion of different biomass as

part of an assistance system for emission reduction. 2019;250:168-75.

13) Madanayake BN, Gan S, Eastwick C, Ng HKJFPT. Biomass as an energy source in coal co-firing and its feasibility enhancement via pre-treatment techniques. 2017;159:287-305.
14) Phung QH, Sasaki K, Sugai Y, Maneeintr K, Tayfun B. Numerical simulation of co2 enhanced coal bed methane recovery for a vietnamese coal seam. 2010.
15) Bandara JC, Jayarathna C, Thapa R, Nielsen HK, Moldestad BM, Eikeland MSJCES. Loop seals in circulating fluidized beds–review and parametric studies using CPFD simulation. 2020;227:115917.
16) Opydo M, Kobyłecki R, Dudek A, Bis ZJB, Bioenergy. The effect of biomass co-combustion in a CFB boiler on solids accumulation on surfaces of P91 steel tube samples. 2016;85:61-8.
17) Yang S, Yang H, Zhang H, Li S, Yue GJPT. A transient method to study the pressure drop characteristics of the cyclone in a CFB system. 2009;192(1):105-9.
18) Zhang R, Yang H, Hu N, Lu J, Wu YJPt. Experimental investigation and model validation of the heat flux profile in a 300 MW CFB boiler. 2013;246:31-40.
19) Shaffer F, Gopalan B, Breault RW, Cocco R, Karri SR, Hays R, et al. High speed imaging of particle flow fields in CFB risers. 2013;242:86-99.
20) Basu P, Butler JJAe. Studies on the operation of loop-seal in circulating fluidized bed boilers. 2009;86(9):1723-31.
21) Kim D, Won Y, Hwang BW, Kim JY, Kim H, Choi Y, et al. Loop-seal flow characteristics of a circulating fluidized bed for 3 MWth scale chemical looping combustion system. 2023;274:127271.
22) Li C, Li H, Zhu QJPt. A hydrodynamic model of loop-seal for a circulating fluidized bed. 2014;252:14-9.
23) Kim SW, Kim SDJPT. Effects of particle properties on solids recycle in loop-seal of a circulating fluidized bed. 2002;124(1-2):76-84.
24) Wang P, Lu J, Xing W, Yang H, Zhang MJPt. Impact of loop seal structure on gas solid flow in a CFB system. 2014;264:177-83.
25) Lee DH, Kim D, Won YS, Choi J-H, Joo JB, Ryu H-JJAPT. Flow rate of solids through recycle chamber of loop seal in a circulating fluidized bed. 2023;34(9):104140.
26) Deng B, Zhou T, Zhang Y, Zhang M, Huang Z, Yang HJCES. Hydrodynamic characteristics in the full-loop circulating fluidized bed under load regulation. Part 2: Simulation. 2022;264:118158.
27) Deng B, Zhou T, Zhang Y, Zhang M, Huang Z, Yang HJCES. Hydrodynamic characteristics in the full-loop circulating fluidized bed under load regulation. Part 1: Experimental investigation. 2023;268:118361.
28) Zerobin F, Penthor S, Bertsch O, Pröll TJPT. Fluidized bed reactor design study for pressurized chemical looping combustion of natural gas. 2017;316:569-77.
29) Armatsombat A, Julmon P, Paengpassa CJAPT. Effect of side aeration and bottom aeration of U-type loop seal in a fluidized bed reactor on flow behaviors of solid particles and solid circulation rate. 2024;35(3):104367.
30) Bolland O, Nicolai RJCEC. Describing mass transfer in circulating fluidized beds by ozone decomposition. 2001;187(1):1-21.
31) Fan C, Zhang Y, Bi X, Song W, Lin WJCEJ. Evaluation of downer reactor performance by catalytic ozone decomposition. 2008;140(1-3):539-54.
32) Li D, Zhu J, Ray MB, Ray AKJCes. Catalytic reaction in a circulating fluidized bed downer: ozone decomposition. 2011;66(20):4615-23.
33) Li J, Luo Z-H, Lan X-Y, Xu C-M, Gao J-SJPT. Numerical simulation of the turbulent gas–solid flow and reaction in a polydisperse FCC riser reactor. 2013;237:569-80.
34) Chew JW, Parker DM, Cocco RA, Hrenya CMJCEJ. Cluster characteristics of continuous size distributions and binary mixtures of Group B particles in dilute riser flow. 2011;178:348-58.
35) Xu J, Zhu J-XJCej. Visualization of particle aggregation and effects of particle properties on cluster characteristics in a CFB riser. 2011;168(1):376-89.
36) Kiani A, Sotudeh-Gharebagh R, Mostoufi NJPt. Cluster size distribution in the freeboard of a gas–solid fluidized bed. 2013;246:1-6.
37) Basu P. Combustion and gasification in fluidized beds: CRC press; 2006.
38) Geldart DJPt. Types of gas fluidization. 1973;7(5):285-92.
39) Geldart DJPT. The effect of particle size and size distribution on the behaviour of gas-fluidised beds. 1972;6(4):201-15.
40) Zhou Y, Wang T, Zhu JJCEJ. Investigation on minimum fluidization velocity in a modified Geldart's diagram. 2023;453:139984.
41) Wang Q, Yang H, Wang P, Lu J, Liu Q, Zhang H, et al. Application of CPFD method in the simulation of a circulating fluidized bed with a loop seal Part II—Investigation of solids circulation. 2014;253:822-8.
42) Kim SW, Namkung W, Kim SDJKJoCE. Solids flow characteristics in loop-seal of a circulating fluidized bed. 1999;16:82-8.
43) Basu P, Cheng LJCER, Design. An analysis of loop seal operations in a circulating fluidized bed. 2000;78(7):991-8.